

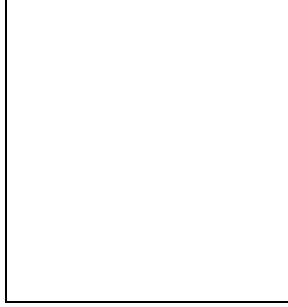
# First Results from ISOCAM Images of Circumnuclear Starbursts in Barred Galaxies <sup>1</sup>

H. Wozniak <sup>1</sup>, D. Friedli <sup>2,3</sup>, L. Martinet <sup>3</sup>, D. Pfenniger <sup>3</sup>

<sup>1</sup> *Observatoire de Marseille, F-13248 Marseille, France.*

<sup>2</sup> *Département de Physique and OMM, Université Laval, Ste-Foy, QC, G1K 7P4, Canada.*

<sup>3</sup> *Observatoire de Genève, CH-1290 Sauverny, Switzerland.*



## Abstract

For a sample of ten nearby barred galaxies, images at  $6.75\mu\text{m}$  and  $15\mu\text{m}$  of circumnuclear starbursts are being taken by ISOCAM on board of the ISO satellite. We first recall the main goals of our project, give its current status, and finally, as an example, preliminary results for NGC 4321 (M100) are presented.

## 1 Introduction

Gravitational perturbations of galaxies are likely to play an important role in generating galaxy starbursts and in fueling active galactic nuclei (AGN). Whereas tidal forces between interacting or merging galaxies are strong enough to drive major gas flows, the compression of which leads to intense starbursts and/or activity in the nuclei, it is less clear whether forming bars alone are also able to trigger enhanced star formation either along the bar or near the centre [8]. NGC 7479 is an example where this activity can be significantly high, the strength of the bar seeming to be an essential parameter to consider [11]. Therefore until recently the link between bar and starburst has not been very clear (see [5] and references therein).

The difficulty with ordering these processes is that they occur on widely different times scales, among which we mention: the bar growth time, the bar life time at its maximum strength, the time scale for driving the gas to the centre, the molecular cloud formation time, the gas cooling time, and finally all the time scales associated with stellar formation and

---

<sup>1</sup> This work is based on observations with ISO, an ESA project with instruments funded by ESA Member States (especially the PI countries: France, Germany, the Netherlands and the United Kingdom) and with the participation of ISAS and NASA.

evolution, such as the energy input from massive stars, the mass return to the interstellar medium from red giants, and the metal enrichment. The involved physics is so complex and some parts so poorly known that only a comparison between simulations and high resolution and multi-spectral observations of the central regions of galaxies can bring some enlightenment on these questions.

One severe issue for feeding AGN is how to accrete gas down to the centre at subparsec scale, which requires a process able to evacuate nearly all the angular momentum. It seems that the same trick to extract angular momentum working well at kpc scale, the bar, can be reused at smaller scales, leading to the often observed secondary bars embedded in the larger one [3]. Such secondary bars can be observed in the visible [1, 16], NIR [14, 4, 2] and CO ([7] and references therein).

Recent star formation needs also a quantitative description. Several attempts have been made to relate the star formation rates to luminosities like e.g.  $L_{H\alpha}$ ,  $L_B$  and  $L_{FIR}$ . However,  $L_{H\alpha}$ , related to recent star formation ( $10^6$  to  $10^7$  yr), is very sensitive to dust absorption while  $L_B$  is more related to  $1 - 3 M_{\odot}$  main sequence stars and thus traces star formation over longer time scales ( $4 \cdot 10^8$  to  $6 \cdot 10^9$  yr). Dust might not only be heated by young massive stars but also by older stars so that  $L_{FIR}$  (estimated from  $60\mu m$  and  $100\mu m$  IRAS measurements) remains a controversial tracer of recent star formation [12].

MIR wavelengths ( $5-17\mu m$ ) trace the hot dust associated with the most recent star formation [15], and thus might give powerful indicators of star formation activity. Indeed, broad band imaging allows to distinguish between the various sources of MIR luminosity (PAHs, graphite grains, etc.). Location of sources of heating can be done at shorter wavelengths. Moreover, MIR imaging operate with larger arrays and better resolution than those available so far in the FIR allowing thus to investigate in a much more detailed way the intricate connections between global dynamics and star formation activity.

## 2 Project aims

The broad aim of our ISO program is to clarify the intimate links between bar dynamics and star formation activity in barred galaxies. MIR imaging is indeed particularly powerful for locating the youngest star forming regions and for exploring broader issues like the dynamical origin of these activities. Among the sites of high star formation activity, the nuclear and/or circumnuclear regions have particularly hold our attention. We thus decided to observe the emission from PAHs and hot dust with the highest pixel field of view ( $PFOV=1.5''px^{-1}$ ) allowed by the ISOCAM camera of the ISO satellite. The small field of view ( $45''$ ) is sufficient to enclose the circumnuclear star forming regions of nearby barred galaxies.

Specific goals include: the analysis of PAHs and hot dust distributions and patterns, the study of gradients in the PAHs/dust ratio, the emphasis of spatial correlations or offsets between various physical components (e.g. young and old stars, molecular and ionized gas, PAHs, dust), the comparison of star formation rates estimated from MIR emission with other indicators, etc.

## 3 Sample and observations

We have selected a sample of ten nuclear and circumnuclear starburst galaxies for which low resolution MIR (e.g. [15]) and/or millimeter maps have been done (cf. Table 1). All these galaxies show signatures generally associated with prominent star formation activity, like  $H\alpha$  emission (e.g. HII regions, hot spots), dust lanes, mini-spirals, nuclear bar and/or ring, etc.

Table 1: Galaxy sample

Objects	Morphological type	Characteristics
<i>Observed (until 31 May 1997):</i>		
NGC 1097	SB(s)b	Seyfert; H $\alpha$ ring
NGC 4321	SAB(s)bc	Mild starburst; H $\alpha$ ring
NGC 5236	SAB(s)c	Starburst; H $\alpha$ ring
NGC 7469	(R')SAB(rs)a	Seyfert; Starburst
NGC 7479	SB(s)c	LINER; Starburst
NGC 7552	(R')SB(s)ab	Starburst
<i>Pending:</i>		
NGC 1808	(R)SAB(s)a	Seyfert
NGC 2903	SAB(rs)bc	Starburst
NGC 3351	SB(r)b	Starburst; H $\alpha$ ring
NGC 4691	(R)SB(s)0/a	H $\alpha$ ring

The ongoing observations (Table 1) were done with the LW2 ( $6.75\mu\text{m}$ ) and LW3 ( $15\mu\text{m}$ ) broad band filters at the  $1.5''\text{px}^{-1}$  PFOV. The beamswitching mode with 2 reference fields was used to remove the MIR background. This program requires roughly 12 hours. Its main difficulty is to deconvolve the image PSF in order to get the best details which should then be compared with the millimetric interferometric maps and data at various other wavelengths. Further details on the reduction and calibration processes can be found in [17].

The LW2 filter ( $5\text{--}8.5\mu\text{m}$ ) includes emission from the PAH bands at  $6.2\mu\text{m}$ ,  $7.7\mu\text{m}$  and  $8.6\mu\text{m}$  as well as the underlying continuum. The LW3 filter ( $12\text{--}18\mu\text{m}$ ) collects continuum emission of small grains as well as [NeII] ( $12.8\mu\text{m}$ ) and [NeIII] ( $15.5\mu\text{m}$ ) emissions if present.

## 4 A puzzling example: NGC 4321 (M100)

NGC 4321 (M100) is a Virgo giant moderately barred spiral galaxy. Its inner region has been extensively studied at almost all wavelengths (see [9, 13] and references therein). Optical, H $\alpha$ , NIR and CO images have revealed many intricate features in the central kpc associated to its mild star formation activity. Several HII regions lie along a 1 kpc circumnuclear ring which crosses a bar 8 kpc long. A nuclear bar, nearly parallel to the large-scale bar, occupies the region inside the ring. In fact, this galaxy certainly represents one of the best laboratory for exploring the interplay between starburst activity and non-axisymmetric dynamics.

At  $6.75\mu\text{m}$  and  $15\mu\text{m}$ , the emission is clearly dominated by two bright spots located near the nuclear bar ends (Fig. 1). These peaks are almost twice brighter than the remainder of the circumnuclear region. A third local maximum, much less intense, is visible at the nucleus. Without any deconvolution, firm morphological differences between LW2 and LW3 images cannot be displayed. Furthermore, the bar-like feature which seems to connect the two peaks and the nucleus must be confirmed on deconvolved images. [17] have performed a detailed analysis of these ISOCAM images and have compared them with U, B, R, H $\alpha$  and CO data. Their main findings are summarized below. A very schematic view of the central multi-wavelength morphology is given in Fig. 2.

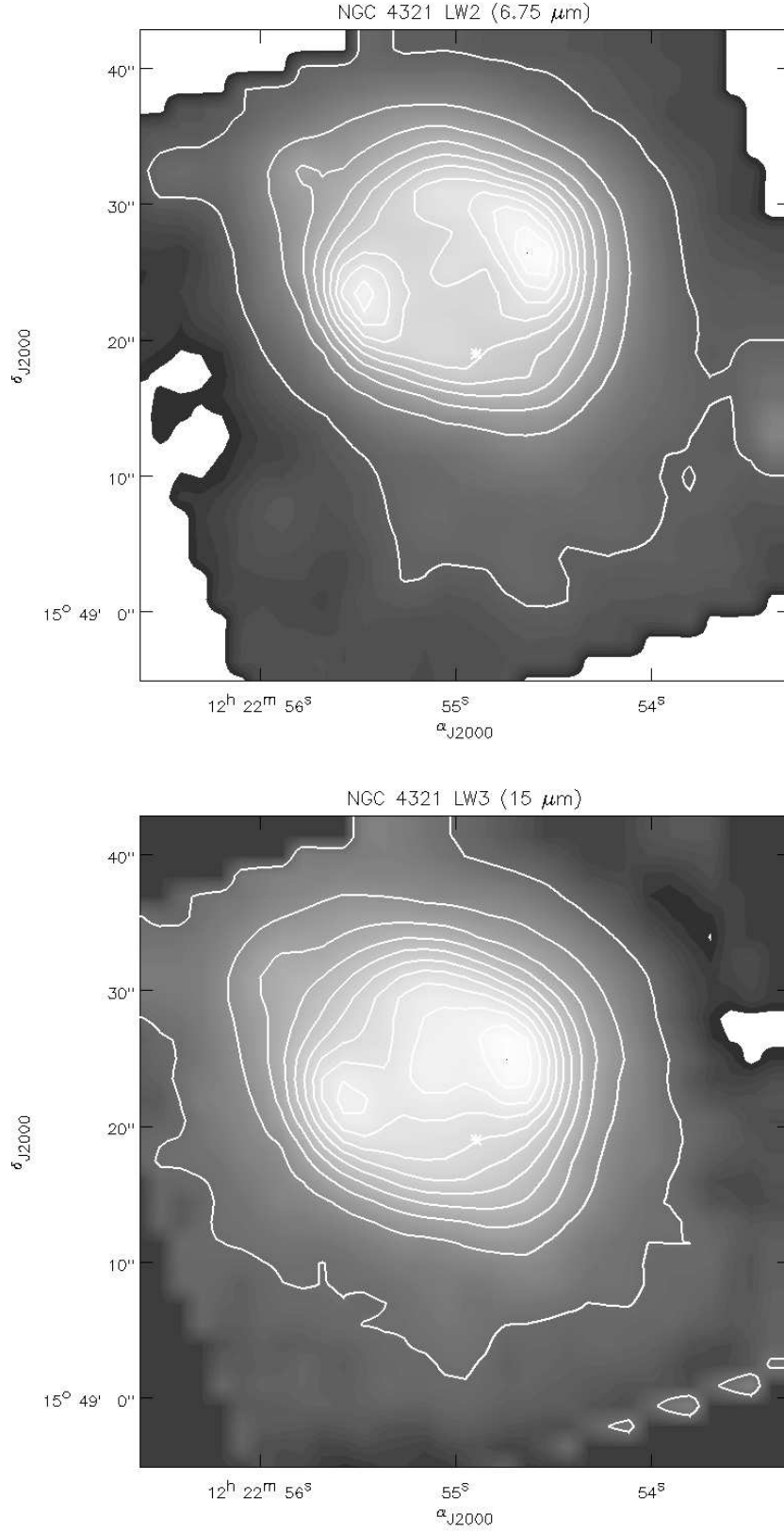


Figure 1: Linear greyscale images of NGC 4321 (M100) at  $6.75\mu\text{m}$  (*top panel*) and  $15\mu\text{m}$  (*bottom panel*). Isocontours spaced by  $0.13 \text{ mJy arcsec}^{-2}$  at  $6.75\mu\text{m}$  and  $0.12 \text{ mJy arcsec}^{-2}$  at  $15\mu\text{m}$  are overplotted. The faintest levels are 0 in both images. The highest ones are  $1.33 \text{ mJy arcsec}^{-2}$  at  $6.75\mu\text{m}$  and  $1.20 \text{ mJy arcsec}^{-2}$  at  $15\mu\text{m}$ . The PFOV is  $1.5'' \text{ px}^{-1}$ . The effective field of view is  $45''$ . The images are not deconvolved.

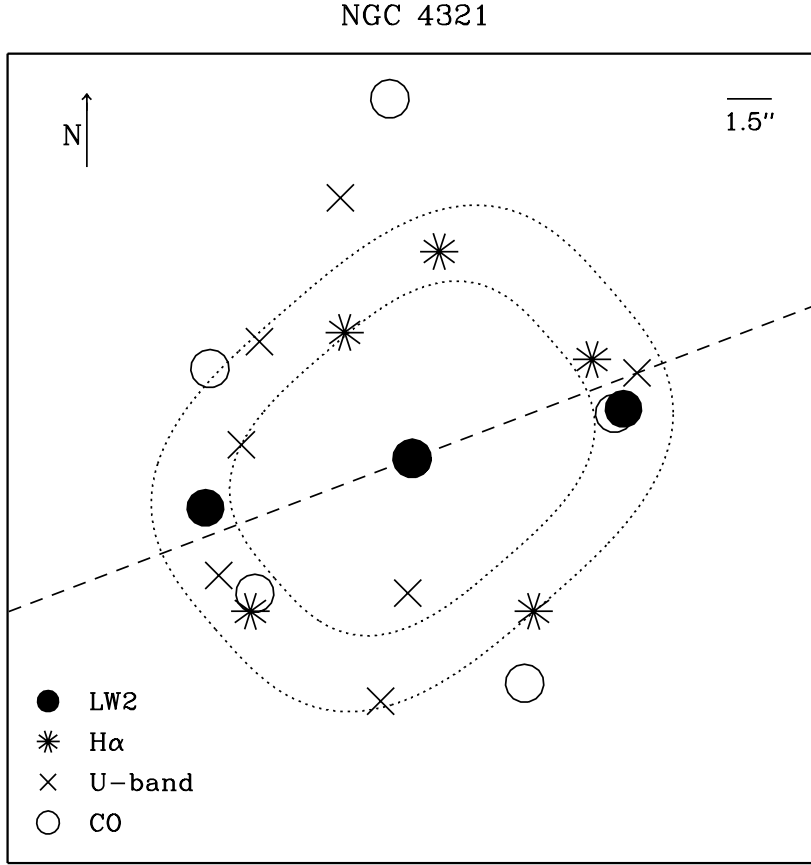


Figure 2: Very schematic sketch of the intricate central morphology of NGC 4321 (M100) including the three LW2 peaks, the direction of the nuclear bar (dashed line; PA= 111° [9]), the position of i) the nuclear H $\alpha$  ring (dotted lines; PA= 131°) with its five most prominent peaks, ii) five regions with intense CO emission, and iii) seven bright regions in U-band.

1) The two bright MIR (i.e. LW2 and LW3) peaks at the nuclear bar ends approximately coincide with strong H $\alpha$  and K-band emissions, dust lanes obscuring optical emission (from U- to I-bands), and similar peaks in CO emission. Moreover, LW2/LW3 > 1 in these regions which may mean that PAHs dominate the MIR luminosity.

2) With respect to the nuclear bar (counter-clockwise rotation), the two MIR maxima are trailing whereas the two H $\alpha$  maxima are leading.

3) The two other regions of star formation (visible in U, B and H $\alpha$  along the nuclear bar minor axis) are not embedded in dust lanes, are offset from the CO spiral arms, and seems not to be associated (or only marginally), neither with a strong emission in NIR, nor with LW2 and LW3 bands. In these regions, the hot dust dominates the MIR emission as LW2/LW3 < 1.

4) There are no “holes” in the LW2 and LW3 surface brightness, i.e. emission from PAHs and hot dust is observed everywhere in the central region. Of course, this might be due to the map resolution which induces a 200 pc wide smoothing.

**Acknowledgements.** We are grateful to Dr. A. Zavagno for enlightening discussions on PAHs. The project is supported by the Swiss National Science Foundation (FNRS) through an “Advanced Researcher” fellowship to D.F. and the grant 20-49239.96 to L.M. and D.P. Figure 2 makes use of data kindly provided by F. Bresolin (U-band), P. Martin and J-R. Roy (H $\alpha$ ), and R. Rand (CO).

## References

- [1] Buta R., Crocker D.A., 1993, *Astron. J.* **105**, 1344
- [2] Combes F., 1997, *this meeting*
- [3] Friedli D., Martinet L., 1993, *Astr. Astrophys.* **277**, 27
- [4] Friedli D., Wozniak H., Rieke M., Martinet L., Bratschi P., 1996 *Astr. Astrophys. Suppl. Ser.* **118**, 461
- [5] Hawarden T.G., Huang J.H., Gu Q.S., 1996 in *Barred Galaxies*, IAU Coll. no 157, ASP Conf. Ser. Vol. 91, R. Buta, D.A. Crocker, B.G. Elmegreen (eds.), p.54
- [6] Huang J.H., Gu Q.S., Su H.J., et al., 1996, *Astr. Astrophys.* **313**, 13
- [7] Kenney J.D.P., 1996, in *Barred Galaxies*, IAU Coll. no 157, ASP Conf. Ser. Vol. 91, R. Buta, D.A. Crocker, B.G. Elmegreen (eds.), p.150
- [8] Kennicutt R.C., Schweizer F., Barnes J.E., 1997, in *Galaxies: Interactions and Induced Star Formation*, Saas-Fee Advanced Course 26, D. Friedli, L. Martinet, D. Pfenniger (eds.). Springer-Verlag, Heidelberg, *in press*
- [9] Knapen J.H., Beckman J.E., Heller C.H., Shlosman I., de Jong R.S., 1995, *Astrophys. J.* **454**, 623
- [10] Lawrence A., Rowan-Robinson M., Leech K., Jones D.H.P., Wall J.V., 1989, *MNRAS* **240**, 349
- [11] Martinet L., Friedli D., 1997, *Astr. Astrophys.* , *in press*
- [12] Sauvage M., Thuan T.X., 1992 *Astrophys. J.* **369**, L69
- [13] Sakamoto K., Okumura S., Minezaki T., Kobayashi Y., Wada K., 1995, *Astron. J.* **110**, 2075
- [14] Shaw, M.A., Combes, F., Axon, D.J., Wright, G.S., 1993, *Astr. Astrophys.* **273**, 31
- [15] Telesco C.M., Dressel L.L., Wolstencroft R.D., 1993, *Astrophys. J.* **414**, 120
- [16] Wozniak H., Friedli D., Martinet L., Martin P., Bratschi P., 1995, *Astr. Astrophys. Suppl. Ser.* **111**, 115
- [17] Wozniak H., Friedli D., Martinet L., Pfenniger D., 1997, *Astr. Astrophys.* , *submitted*